

Department of Meteorology and Supercomputer Computations Research Institute, Florida State University, Tallahassee, U.S.A.

## **Energy Transports by Ocean and Atmosphere Based on an Entropy Extremum Principle. Part II: Two-Dimensional Transports**

**B.-J. Sohn\*** and **E. A. Smith**

With 7 Figures

Received December 28, 1992  
Revised May 3, 1993

### **Summary**

The maximum entropy production (MEP) principle used in Part I has been extended to separate the two-dimensional required energy transports determined from Nimbus 7 satellite net radiation measurements into atmospheric and oceanic components. In terms of the meridional component of the ocean transport vectors, results show northward ocean transports throughout the entire Atlantic ocean from southern hemisphere high latitudes to northern hemisphere polar regions, southward transports throughout the entire Indian Ocean, and poleward transports separated at approximately  $10^{\circ}$  S in the Pacific Ocean. The ocean transport patterns are consistent with well-known features concerning heat transport within the three ocean basins. However, uncertainty remains in the magnitudes of the transports. Because of the large remaining discrepancies between published estimates based on direct measurements and indirect estimates derived from energy budget methods, assessing the accuracy of the magnitudes is difficult, although there is evidence that the limited model resolution leads to synergistic biases in the North Atlantic and North Pacific. In terms of the cross-meridional energy transport component, results suggest that most of the net energy transfer in the tropics takes place within the ocean. In the southern hemisphere high latitudes, the Pacific and Indian Oceans export heat cross-meridionally to the Atlantic Ocean through the passages below Cape Horn and the Cape of Good Hope, although the magnitudes of these inter-ocean heat exchanges are small. Another important aspect of the southern hemisphere results is that

poleward transports are dominated by the atmospheric component with strong zonal asymmetry. By contrast, in the northern hemisphere, atmospheric transports over the ocean are generally weaker than the corresponding southern hemisphere terms, indicating that the northern hemisphere oceans are relatively more effective in transferring heat poleward. Finally, poleward atmospheric transports over the continental areas exceed those over the ocean at equivalent latitudes as a result of the generally greater energy deficits over the land areas.

### **1. Introduction**

Satellite measurements of the radiation flux at the top of the atmosphere (TOA) have long revealed that imbalances between absorbed solar radiation and emitted infrared radiation produce apparent energy surplus in the tropics and energy deficit in high latitudes. Such an imbalance gives rise to poleward transports of heat on a global scale, transports that must take place within both the atmosphere and ocean. Traditionally, global heat transports in the two fluids have been examined in a one-dimensional zonal-averaged framework. The problem with such an approach is that it overlooks the significant zonal structures intrinsic to the process, particularly in the tropics. A recent study of Sohn and Smith (1992a) emphasizes the importance of east-west transports. They have shown that the cross-meridional heat flux is about 30% of the meridional component in the tropics

---

\* Current Affiliation: Universities Space Research Association, NASA/Marshall Space Flight Center, ES42, Huntsville, AL 35812.

and that a major feature of the tropical radiation climatology is an east-west coupled dipole pattern of cross-meridional energy transport associated with significant zonal gradients in the net radiation field induced by land-sea contrasts and variations in large scale cloudiness distribution. This is the compelling evidence, from a radiation budget perspective, why we contend that climatic changes over the tropics are strongly associated with east-west coupled phenomena; see Sohn and Smith (1992b). Thus, a two-dimensional approach leads to a better understanding of the basic climatic behavior associated with atmosphere and ocean energy transfer. However, to date, conventional measurements of global dynamic and thermodynamic variables do not permit the direct calculation of reliable, two-dimensional, atmospheric and oceanic energy transports.

Campbell (1980) obtained two-dimensional oceanic divergence of energy by differencing the explicit atmospheric divergence of heat fluxes (using general circulation statistics) from measured net radiation, but his approach led to implausible ground flux divergences over land. In that study, the ground flux divergences were of about the same magnitude as those of the atmosphere, which detracted from the reliability of the oceanic energy transport estimates. An implicit method was used by Paltridge (1978). He calculated two-dimensional atmospheric and oceanic transports by applying an extremum principle of maximum entropy production (MEP) to the earth-atmosphere system, demonstrating that his approach resolved some known dynamic phenomena – e.g. the Gulf Stream, Kuroshio and East-Australian current. However, the basic heat transport patterns were much different from generally known features; atmospheric and oceanic energy divergences were less than half the magnitude suggested by satellite measurements and the ocean transports mimicked the total opposing poleward transports in all three ocean basins with the zero transport contours lying near the equator. Since the problems with this result were never actually resolved, there has been a long-standing debate over the wisdom of using extremum principles in models of the earth's climate. The review of North et al. (1981) discusses the use of extremum principles in energy balance models; Part I of this paper (Sohn and Smith, 1983) summarizes the debate on the application of extremum principles on global thermodynamics.

In the Part I paper, we first investigated the MEP technique in a one-dimensional scalar framework to demonstrate that the generally accepted features of the zonal-averaged transport field could be reproduced. These results suggested that the MEP principle could serve as a governing rule on macroscopic global climate. The model was then extended to two dimensions to determine if the averaged meridional ocean transports within the three separate ocean basins (partial zonal-averages) could be realistically diagnosed from the vector solution. Comparison of these results to direct and indirect estimates verified that the main features of hemispherically distributed poleward transports could be reproduced, i.e. northward transports throughout the entire Atlantic basin, southward transports throughout the entire Indian ocean, and separate poleward transports in the north and south hemispheres of the Pacific ocean. The current paper extends the two-dimensional modeling methodology to analyze specific features of the zonal and meridional components of the vector solution, including more detailed examination of the nature of cross-meridional energy transports in both atmosphere and oceans.

## 2. Description of Two-Dimensional Model

In Part I, the MEP principle was used with the total required transport field derived from Nimbus 7 satellite radiation budget data to separate the solution into zonal-averaged oceanic and atmospheric quantities. Most of modeling procedures used in this study are unchanged from Part I, but for convenience, the calculation methodology is summarized including a brief introduction of the MEP principle.

In a non-equilibrium state, the time rate of change of global entropy ( $dS/dt$ ) is a function of entropy production due to irreversible processes within the interior ( $dS_i/dt$ ), and of entropy exchange ( $dS_e/dt$ ) with the system's environment, i.e.:

$$\frac{dS}{dt} = \frac{dS_i}{dt} + \frac{dS_e}{dt}. \quad (1)$$

At steady state, the global entropy is constant and thus the internal production is balanced by the export of entropy so that:

$$\frac{dS_i}{dt} = - \frac{dS_e}{dt}. \quad (2)$$

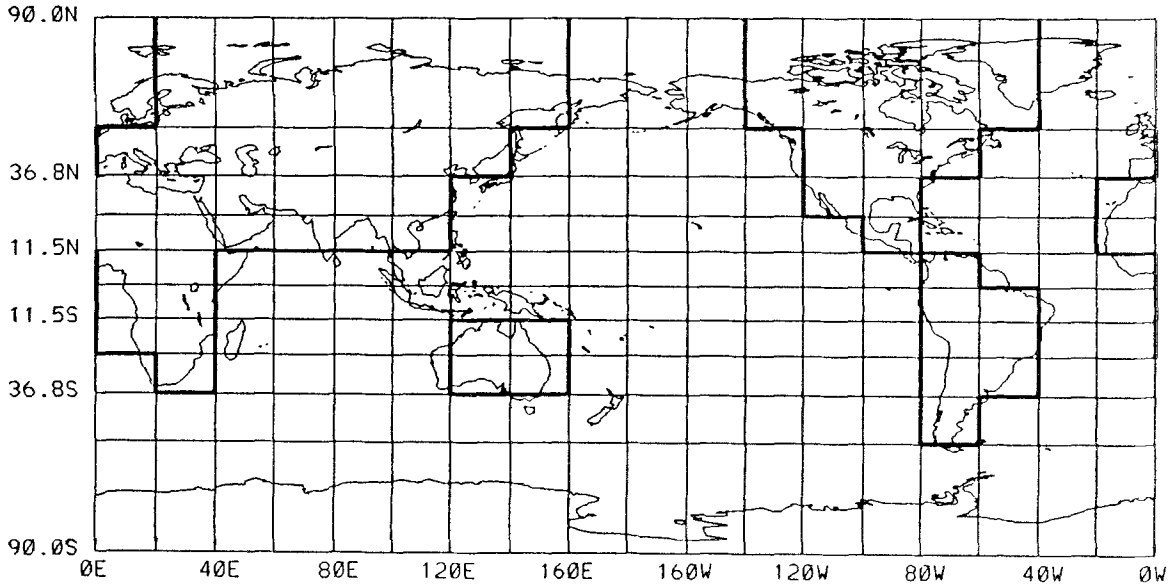


Fig. 1. Domain of the equal area 180 box model. Bold lines are the implied continental outlines across which oceanic energy flux is not allowed

The MEP principle states that entropy production due to irreversible processes is at a maximum within the earth-atmosphere system under the assumption that the system undergoes a form of non-linear steady state in the long term mean.

In order to decompose the total transport solution into two-dimensional atmospheric and oceanic terms, the globe is divided into 180 equal area boxes over a two-dimensional domain for which the MEP principle is applied to the atmosphere. A schematic of the grid mesh is shown in Fig. 1. The bold lines indicate the prescribed continental boundaries which do not allow the penetration of heat by oceans. Each box consists of two sub-systems (atmosphere and ocean) such that energy balance is achieved at each grid box of each sub-system. Atmospheric energy balance of each box requires that:

$$Q^* - Q_s^* + (QE + QH) - \nabla \cdot X^a = 0 \quad (3)$$

with the associated oceanic energy balance given by:

$$Q_s^* - (QE + QH) - \nabla \cdot X^o = 0. \quad (4)$$

In Eqs. (3) and (4),  $Q^*$  and  $Q_s^*$  denote net radiation energy received at the TOA and surface respectively,  $(QE + QH)$  the total turbulent heat flux, and  $X^a$  and  $X^o$  the two-dimensional energy fluxes by

atmosphere and ocean, respectively. In this study we adopt Paltridge's energy balance model in which  $Q^*$ ,  $Q_s^*$ , and  $(QE + QH)$  are parameterized using surface temperature ( $T$ ) and cloud amount ( $A_c$ ). The parameterized and various latitudinally dependent constants used in the model are found in Paltridge (1975); clear sky albedo is obtained from the area mean of the Nimbus 7 narrow-field-of-view estimates of this parameter at each grid box.

There are four unknowns ( $T$ ,  $A_c$ ,  $X^a$ , and  $X^o$ ) in the two energy balance equations. In order to solve the equations, the oceanic fluxes (or atmospheric fluxes) are assigned as the unknown variables. The corresponding atmospheric fluxes (or oceanic fluxes) are determined by subtraction from the total flux since the total energy transport requirement ( $X^t$ ) is the sum of the atmospheric and oceanic components and the  $X^t$ 's are diagnosed directly from the satellite net radiation measurements.

The north-south and east-west components of the required transports are obtained by using the concept of a steady state radiation climate represented by a long term mean of net radiation. Here we use five-year mean net radiation from 1979 to 1983 measured by the Nimbus 7 satellite. The energy balance of the earth-atmosphere system at

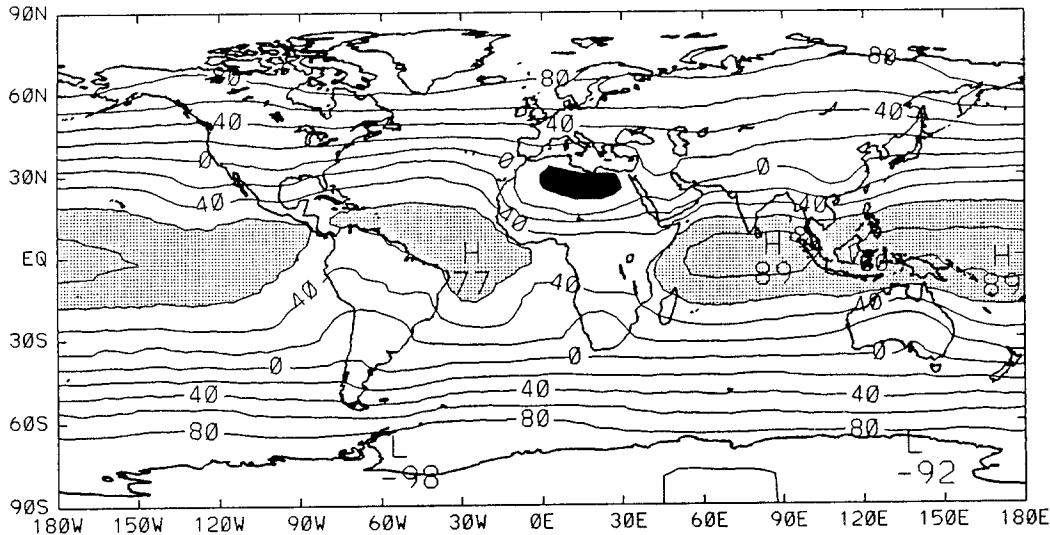


Fig. 2. Global distribution of the five year (1979–1983) mean net radiation flux at the top-of-atmosphere in  $\text{W m}^{-2}$  using a  $20 \text{ W m}^{-2}$  contour interval. Areas whose fluxes are larger than  $60 \text{ W m}^{-2}$  shaded. Black shading indicates the North African deficit region

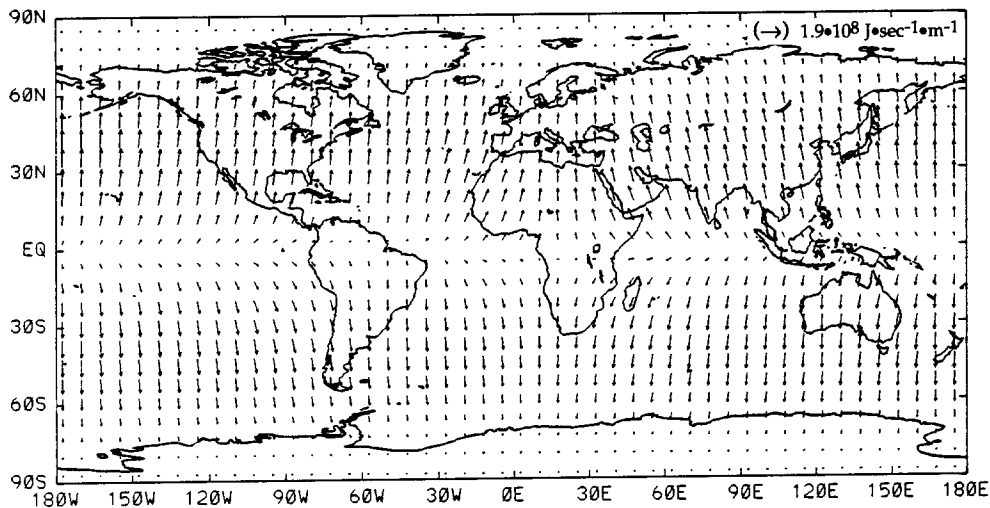


Fig. 3. Five year (1979–1983) mean required vectorial two-dimensional transports. The maximum vector magnitude is  $1.9 \cdot 10^8 \text{ J sec}^{-1} \text{ m}^{-1}$  (a reference arrow of this magnitude is shown in the upper right corner of the diagram)

given box is obtained by adding Eqs. (3) and (4):

$$Q^* = \nabla \cdot (X^a + X^o) = \nabla \cdot X^t. \quad (5)$$

Separating the total energy flux ( $X^t$ ) into rotational ( $X^t_R$ ) and divergent ( $X^t_D$ ) parts based on the Helmholtz theorem, Eq. (5) becomes:

$$Q^* = \nabla \cdot X^t_D = -\nabla \cdot \nabla \Phi \quad (6)$$

where  $\Phi$  is the energy transport function. From the distribution of net radiation given in Fig. 2,

we solve the Poisson Eq. (6) for  $\Phi$  using spherical harmonics. The divergent part of energy transport is then obtained by taking derivatives of  $\Phi$ . The calculated total energy transport field is given in Fig. 3. Additional discussion of these calculations and their implications for climate are found in Sohn and Smith (1992a).

The diagnosed meridional and zonal transports of ( $X^t_D$ ) are imposed as a constraint so that the sums of atmospheric and oceanic flux divergences are

equal to the net radiation measurements within a certain error tolerance. For specified meridional and zonal required fluxes within the ocean and atmosphere, the two unknowns ( $T$  and  $A_c$ ) can be determined. The atmospheric temperature ( $T_a$ ) for the calculation of entropy production in the atmosphere is then obtained by a gray body relationship with respect to the thermal infrared flux emitted at the top-of-atmosphere. There may be an infinite set of atmospheric-oceanic heat flux distributions which both satisfy the model and achieve a steady state configuration. To find the unique set of fluxes which yield global maximum entropy production within the atmosphere, the entropy functional is optimized such that each box has three degrees of freedom – surface temperature, cloud amount, and energy flux within either atmosphere or ocean. Inequality constraints are employed in the variational solution to allow  $\pm 5\%$  error in the net radiation measurements (corresponding to an  $\approx \pm 3 \text{ W m}^{-2}$  uncertainty at tropical latitudes). Since  $T_a$  can be diagnosed at each box, we can seek a set of atmospheric and oceanic transports that achieve both maximum entropy production within the atmosphere and satisfy the total transport requirements. As in the one-dimensional solution, equal energy dissipation estimates are applied to obtain an initial guess field. During the optimization, a further inequality constraint is employed involving the ratios of the zonally integrated northward oceanic transports to the totals obtained in Part I, keeping the ratios within a prescribed interval around those found for the one-dimensional model. Additional details on the optimization procedures are found in Appendices A and B of Part I. The optimization is applied only over oceans since heat transports within the land masses are negligible on an interannual basis and thus the total required transports are induced by the atmosphere alone.

### 3. Results

The geographical distribution of surface temperatures which satisfies MEP in the atmosphere are presented in Fig. 4a. The general features are in good agreement with climatological observations, with the exception of two localized areas off the west coasts of South America and South Africa where the model derived temperatures exceed  $30^\circ\text{C}$ , some 6–10 degrees higher than climatology.

These discrepancies over the coastal upwelling zones are due to the use of latitudinal mean properties for cloud effects on the radiation field. The persistent marine stratus cloud decks over the upwelling zones exhibit a much larger impact on shortwave radiation than on longwave radiation, i.e. there are relatively small differences in temperature between cloud top and surface (see Sohn and Smith, 1992c). Because of these specific cloud-radiative properties the coastal zones generally exhibit larger values of emitted longwave radiation than the associated zonal mean. Thus, the zonally averaged cloud properties employed in the model give rise to less longwave emission than what actually takes place. In order to attain maximum atmospheric entropy production consistent with the relatively larger values over these regions, the model atmosphere obtains the larger emitted fluxes through larger surface temperatures.

Lesser discrepancies in surface temperature are found along the coasts in the northern hemisphere, in particular, over the western boundary current regions where the model does not reproduce the strong temperature contrasts. Part of this is due to the fact that the prescribed continental boundaries treat portions of the boundary current areas as land, an unavoidable outcome of choosing a 180-box grid mesh. In addition, the spatial resolution of the model itself blurs details in the temperature patterns, and represents another source of error. A higher resolution model would likely eliminate some of these discrepancies, however the computational requirements would become substantial.

The model generated cloud amount distribution is given in Fig. 4b along with a six-year mean observational result derived from the Nimbus 7 cloud climatology. The general pattern is in good agreement with the satellite estimates in keeping with the one-dimensional results of Part I. In terms of magnitude, the model underestimates the cloud amount with respect to observations in tropical latitudes, however the differences are within the uncertainty limits of satellite based cloud retrieval (W. Rossow, personal communication, 1992). More cloudiness is found over northern hemisphere continents than over oceanic areas at the same latitude, in contrast to the observations which show the opposite relationship. Considering that the optimization procedure is only applied over ocean areas and the solutions

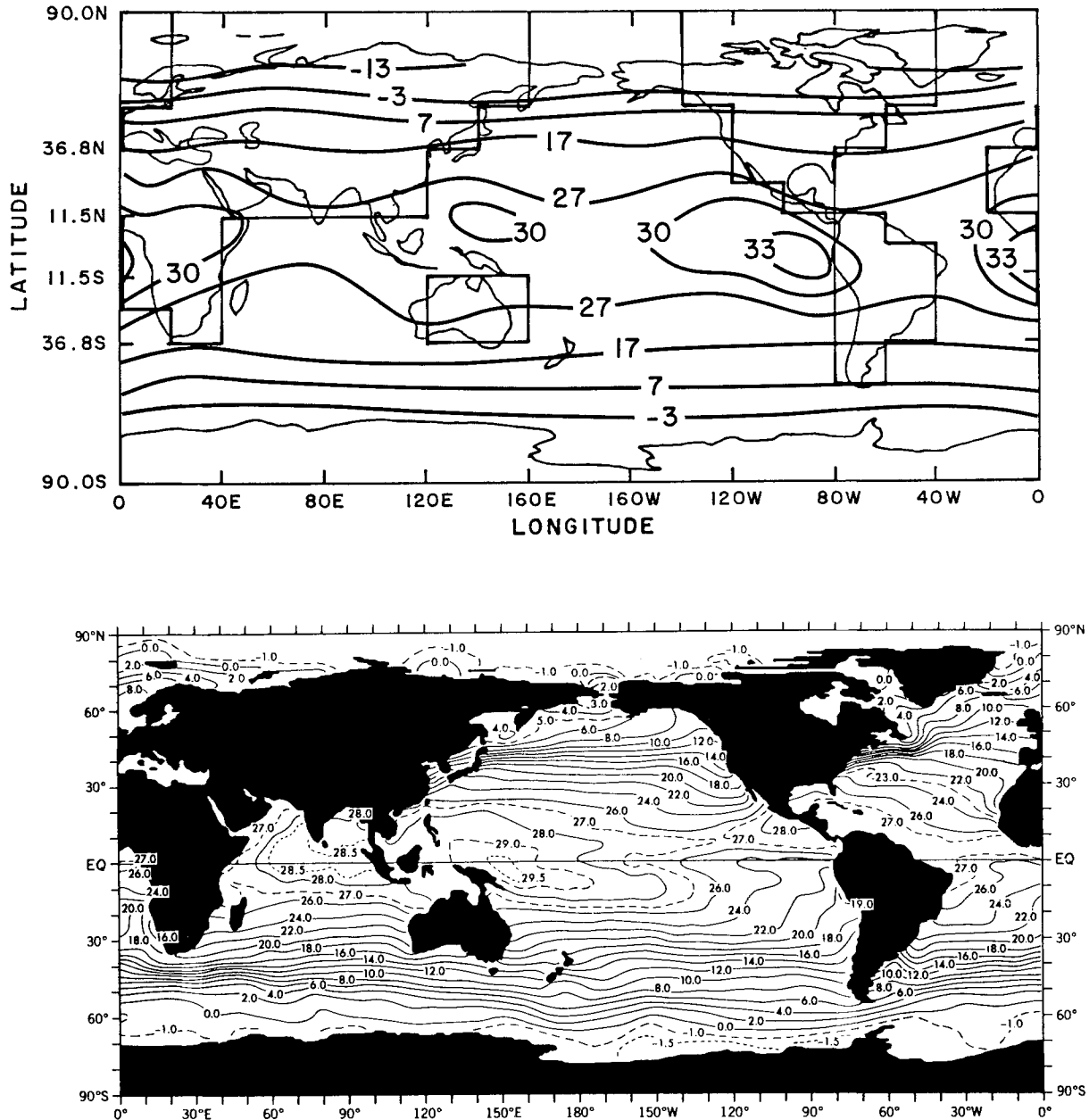


Fig. 4a. Global distribution of model estimated (top) and observed (bottom) (Levitus, 1982) surface temperature. Units are in  $^{\circ}\text{C}$

over continental areas are directly determined by requiring equivalence between atmospheric and total transports, these discrepancies indicate shortcomings in the physics of the model.

Because discrepancies in the temperature and cloud distributions are indicative of uncertainties in the derived transports, we originally conducted a number of sensitivity tests concerning how model parameters affect transport results on a zonal mean basis (see Table 2 of Part I). From these tests we found that the ocean heat transports are not highly sensitive to nominal variations in physical

parameters in the model, except for the solar constant, in comparison to temperature and cloud amount sensitivities. In fact, 10% increases in the tested parameters (except for the solar constant) lead to less than  $1 \times 10^{14} \text{ W}$  changes in zonal mean meridional transport. Thus, although improved physical parameterizations in the model could bring about better agreement with the observed surface temperature and cloudiness observations, they would not necessarily improve the accuracy of the required transport field. The difficulty with this issue is that there is no currently

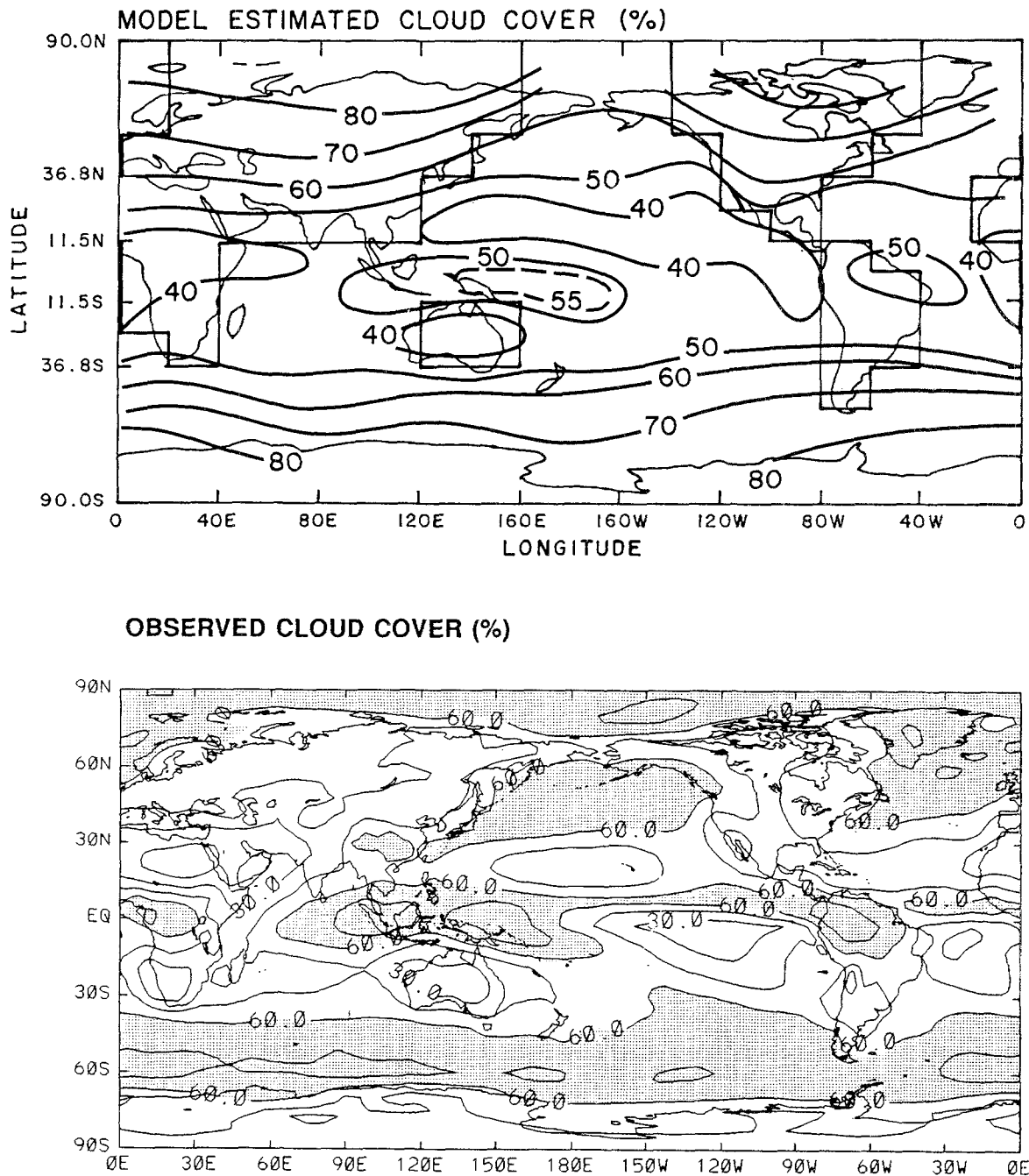


Fig. 4b. Global distribution of model estimated and Nimbus 7 observed (Stowe et al., 1988) cloud amount. For observed cloud cover, shading represents values larger than 60%.

reliable means to assess the accuracy of such estimates, particularly with respect to the ocean term.

The model generated oceanic heat transports are given in Fig. 5a. The Indian Ocean shows general flux divergence in low latitudes with convergence in high latitudes, and thus overall heat transport directed towards the south with magnitudes from  $-1.8 \cdot 10^{14}$  W to  $-6.9 \cdot 10^{14}$  W;

the maximum occurs in the vicinity of  $11.5^\circ$  S (see Table 1). As seen in Table 1, the direction of the basin-averaged transports of the new results are in good agreement with most direct estimates (Fu, 1986; Toole and Raymer, 1985; Georgi and Toole, 1982). Bennett's (1978) results show large equatorward transports at  $40^\circ$  S, however, his data set may have been too small to be representative of the basin scale. Magnitudes are more difficult to

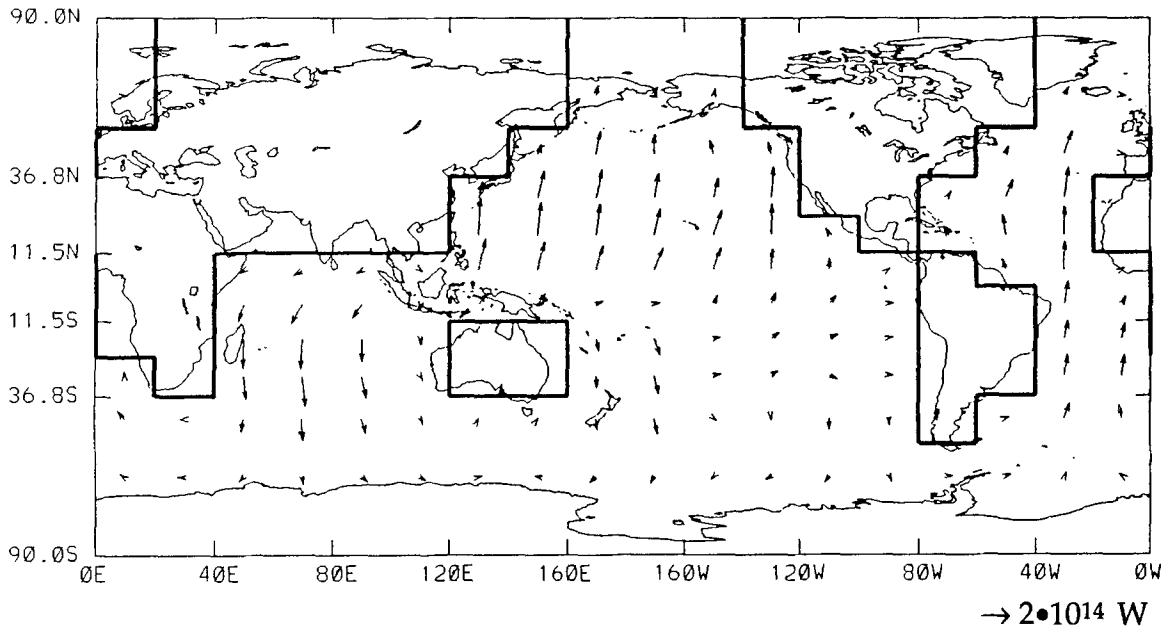


Fig. 5a. Vectorial two-dimensional oceanic energy transports. A reference arrow is presented at the bottom of the diagram in units of  $10^{14}$  W

Table 1. Meridional Energy Transports (in  $10^{14}$  W) for Indian Ocean

Lat	This study	*Fu (1986)	*Toole and Raymer (1985)	*Georgi and Toole (1982)	*Bennett (1978)	@Hsiung (1985)	@Hastenrath (1982)
Eq	-1.8					-7.9	-4.8
11.5° S	-6.9						
15° S	-6.9					-15.8	-7.7
18° S	-6.8	-6.9					
23.5° S	-6.8						
30° S	-6.2					-14.2	-4.9
32° S	-6.0	-2.5	-8.0 to -4.0				
36.8° S	-5.5						
40° S	-5.1			-8.8 to -6.4	4.6 to 6.4 15.5 to 17.6	-11.4	
53.1° S	-3.3						

\* Direct estimates

@ Indirect estimates

evaluate because of the substantial discrepancies between the published findings. However, with the exception of the Bennett (1978) study, there is general consistency between the new estimates and the direct estimates. Our results are also consistent with the indirect estimates of Hastenrath (1982) in both direction and magnitude, and with the indirect estimates of Hsiung (1985) in terms of direction, although the magnitudes of the latter study are approximately twice the magnitude

found by Hastenrath. Significant low latitude westward heat transports, whose magnitudes are comparable to the north-south transports, take place in the equatorial Indian Ocean as part of an overall Indian Ocean gyre. Clear evidence of inter-ocean heat exchange is found between the Indian and Atlantic Oceans across the Agulhas Retroflexion, indicating that the Indian Ocean, on the whole, exports energy to the Atlantic. It is also noted that there is no clear indication of heat



Table 2. Meridional Energy Transports (in  $10^{14}$  W) for Atlantic Ocean

Lat	This study	*Rago and Rossby (1987)	*Roemmich and Wunsch (1985)	*Hall and Bryden (1982)	*Fu (1981)	*Bennett (1978)	@Hsiung (1985)	@Hastenrath (1982)	@Hall and Bryden (1982)
60° N	0.9						2.4	2.6	1.6
53.1° N	1.1								
50° N	1.5						4.5		4.2
36° N	3.3		8.0						
32° N	3.7	14.0							
30° N	4.0						9.5	10.7	10.7
24° N	4.6		12.0	12.0					
15° N	3.9						8.7	11.1	
11.5° N	3.6								
Eq	2.5						5.4	9.8	7.5
10° S	2.2				1.0 to 2.5				4.9
11.5° S	2.1								
15° S	2.3				6.3 to 8.3		2.0		
20° S	2.6						1.5		5.2
24° S	2.9				4.3 to 6.4	3.4 to 6.5			
30° S	3.5						0.4	6.9	3.9
32° S	3.7				6.6 to 8.8	1.6 to 6.8			
36.8° S	4.1								
40° S	3.6						0.9	6.0	4.3
53.1° S	1.5								

\* Direct estimates

@ Indirect estimates

Table 3. Meridional Energy Transports (in  $10^{14}$  W) for Pacific Ocean

Lat	This study	*Bryden et al. (1991)	*Roemmich and McCallister (1989)	*Wunsch et al. (1983)	*Georgi and Toole (1982)	*Bennett (1978)	@Hsiung (1985)	@Talley (1984)	@Hastenrath (1982)
60° N	3.0						0.0		0.1
53.1° N	3.7								
47° N	5.3		-0.9					-0.5	
36.8° N	8.1								
35° N	8.9		-1.6						
32° N	10.2								
30° N	11.0						5.5	-1.9	11.4
24° N	13.6	7.6	7.5						
20° N	14.0							1.3	
11.5° N	15.0							3.1	
Eq	9.5						3.2	-5.3	-2.3
11.5° S	-1.4							-18.8	
20° S	-1.5						-5.2	-22.6	-20.7
23.5° S	-1.5								
28° S	-2.1			-4.0 to +0.4		-11.6 to -1.7			
30° S	-2.3						-2.4	-22.0	-19.2
36.8° S	-3.2								
40° S	-3.5				-0.9 to +0.4		0.9	-22.2	
43° S	-3.8			-3.8 to +3.2		-1.5 to +4.2			
53.1° S	-4.7								
60° S	-3.8								-11.9

\* Direct estimates

@ Indirect estimates

exchange between the Indian Ocean and Pacific Ocean in low latitudes, consistent with the findings of Blazejewski et al. (1986). Heat exchange between the two ocean basins is found to be negligible at high latitudes. This is in contrast to Hsiung's (1985) result that the Indian Ocean exports energy to both the Atlantic and Pacific.

The Atlantic Ocean transports heat northward throughout the entire basin, consistent with previously published direct and indirect estimates given in Table 2. On the other hand, it is clear that the general magnitude of the new results in the North Atlantic, are smaller than observations. It is difficult to generalize about the magnitudes in the South Atlantic because there is no consistency in the published results. However, if a mean profile is calculated from the five studies that report South Atlantic values in Table 2, those averages compare well with the new results. We suspect the problem in the North Atlantic is mostly due to imperfections in prescribing continental boundaries because of the limited spatial resolution of the grid mesh. For example, the east-west distance of the Atlantic Ocean at  $37^\circ\text{N}$  is nearly half of the actual geographic length (see Fig. 1). Because of the smaller geographical realm apportioned to the ocean, the total meridional transports are smaller by necessity. Furthermore, the Florida

Current and Gulf Stream, where the largest northward heat transports are found (see the heat exchange map of Bunker, 1976), are treated as part of the North America Continent. This leads to even smaller values of total transport by the North Atlantic. Nevertheless, there are clear indications of inter-ocean heat exchange between the Atlantic and Pacific Oceans through the Drake Passage, and between the Atlantic and the Indian Oceans below the Cape of Good Hope consistent with the findings of Hastenrath (1982).

The Pacific Ocean represents the most difficult basin in which to try and reconcile differences, because of the substantial discrepancies between past published results. In essence, we find large northward transports in the North Pacific with a maximum of about  $15 \cdot 10^{14}\text{ W}$  across  $11.5^\circ\text{N}$  latitude, much weaker poleward transports in the southern hemisphere south of  $10^\circ\text{S}$ , and northward transports across the equator. As seen in Table 3, the direct estimates of Bryden et al. (1991) and Roemmich and McCallister (1989) suggest that ocean heat transports across  $24^\circ\text{N}$  in the North Pacific are about  $7.5 \cdot 10^{14}\text{ W}$  northward, which are half the magnitude of the new results. At  $30^\circ\text{N}$ , Hsiung's (1975) indirect estimate is also about half of the new estimate, whereas Hastenrath (1982) reports a value at this latitude similar to

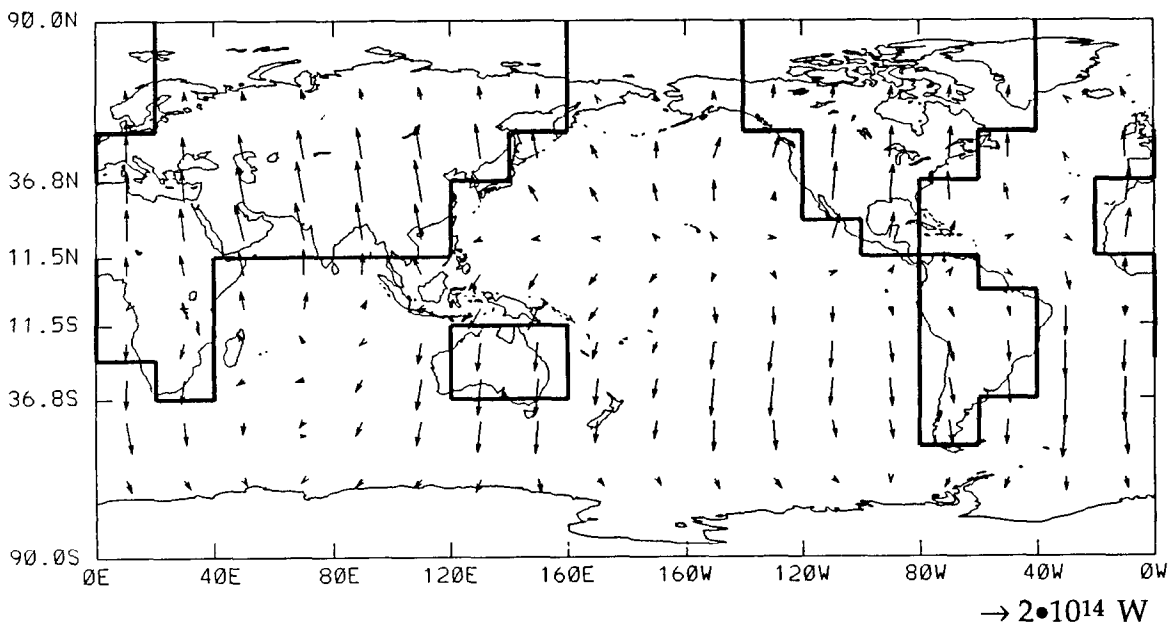


Fig. 5b. Same as Fig. 6 for atmospheric energy transports

ours. There is a good reason to suggest that the new results are too large in the North Pacific. Since the ratios of ocean transports to the associated total required transports obtained in the one-dimensional calculations have been used as optimization constraints, the underestimates in the North Atlantic cloud lead to overestimates in the North Pacific.

In the South Pacific, maximum poleward transports are found at 53° S. In this basin, there have been major disagreements between results from surface heat budget studies and from the direct oceanographic calculations. Wunsch et al. (1983) applied an inverse method to hydrographic data and obtained heat fluxes of  $-1.8 \pm 2.2 \times 10^{14}$  W at 28° S and  $-0.3 \pm 3.5 \times 10^{14}$  W at 43° S, which are consistent with the flux ranges of other direct estimates (Georgi and Toole, 1982; Bennett, 1978). These results are in conflict with those of Hastenrath (1982) and Talley (1984) inferred from indirect methods. However, the indirect calculations of Hsiung (1985) are comparable in magnitude to other direct estimations. In summary, the South Pacific transport results obtained from the MEP method presented here, are most compatible with the direct estimates and those of Hsiung (1985).

The representation of oceanic transports, particularly in the North Atlantic and North Pacific, could be improved by going to higher grid resolution, however, the computational overhead of even a 180-box model is considerable (a single solution at this resolution requires 5 hours of Cray-YMP time). Doubling the resolution of the model requires a four-fold increase in computing time.

The two-dimensional atmospheric transports are given in Fig. 5b. It is noted that there are stronger poleward transports over the northern hemisphere continents than over the oceans, in particular over north central Asia and north central Canada, yielding strong heat convergence over high-latitude land areas. Because the conduction of heat by the solid earth is negligible, we force the required transports over land to be carried out by the atmosphere alone, that is the atmospheric transports over land in this study are equal to the total required transports themselves. Since the divergence of the required transport is equal to the net radiation at the TOA, it is not surprising that the regions of largest heat convergence by the atmosphere are found over high-latitude conti-

ental areas where large negative values of net radiation are observed. It is also noted that these convergence patterns are consistent with the vertically integrated horizontal flow of atmospheric energy by atmospheric eddies based on circulation statistics of dynamic and thermodynamic variables (Oort and Peixoto, 1983).

In the northern part of the Indian Ocean (Eq-20° N), the atmosphere induces relatively strong northward transports, but in the southern hemisphere extratropics, transports are southward and generally weaker than those induced by the ocean. Cross-equatorial energy transport from the southern hemisphere to the northern hemisphere is evident. In contrast, the Pacific and Atlantic Oceans show relatively weak northward transports in the northern hemisphere, but strong southward transports in the southern hemisphere. These distributions induce strong zonal asymmetry in the atmospheric transports in the southern hemispheric extratropics with maximum transports found in the South Atlantic.

One might expect the atmospheric transports in the southern hemisphere to be much more symmetric than in the northern hemisphere as well as exhibiting a maximum in the Indian Ocean, because departures from zonal symmetry in the geopotential height field are smaller than those for the northern hemisphere and maximum atmospheric variability is observed in the Indian Ocean (Trenberth, 1981). However, for heat balance over the southern hemispheric extratropics, the atmosphere must induce strong zonal asymmetries with a maximum in the Atlantic Ocean. This is because the South Atlantic Ocean transports heat directly from the southern hemisphere high latitudes toward the equator (i.e., northward), whereas the Indian Ocean exports heat from the equatorial areas to high latitudes (i.e., southward). This pattern is consistent with the findings of Fu (1981, 1986), Hastenrath (1982), and Hall and Bryden (1982) among others. Consistent with these basic processes, the model produces strong zonal asymmetries in the southern hemisphere. Considering that the high latitudes are areas of net radiation deficit, the heat transports from a deficit region to a surplus region in the South Atlantic Ocean must lead to more of an overall total heat sink. Thus the only way to achieve heat balance at high latitudes in the southern hemisphere is via atmospheric transports which counter the effect of the

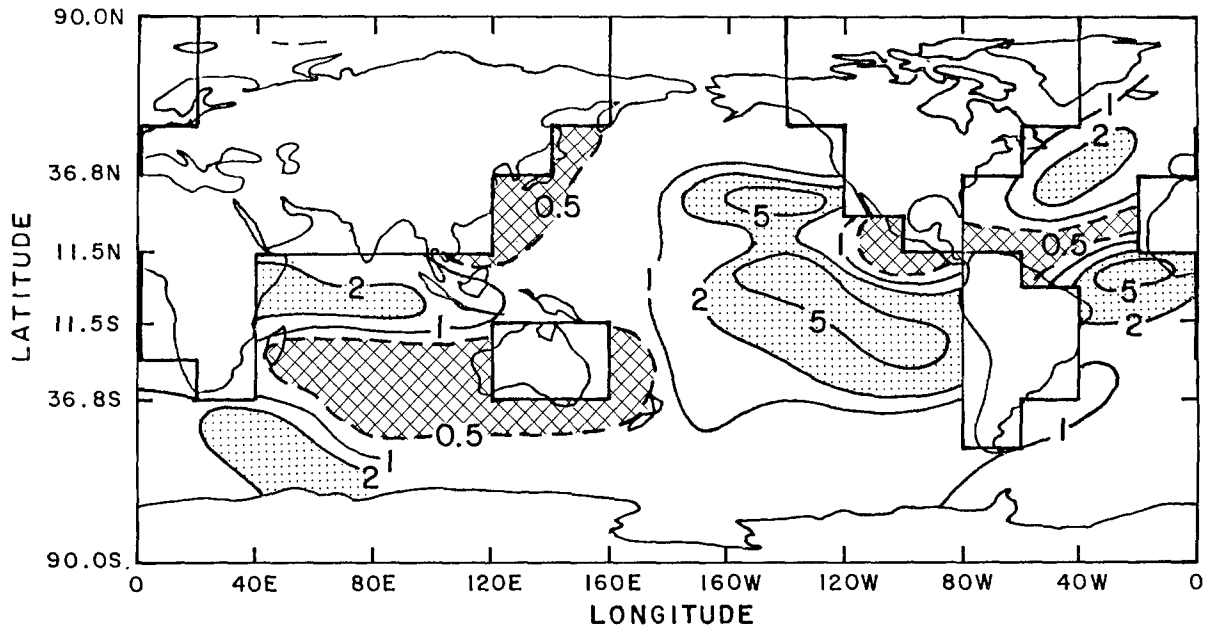


Fig. 6. Ratio of cross-meridional oceanic energy transports to the corresponding atmospheric component. Dotted areas ( $>2$ ) represent oceanic dominance; blank areas ( $0.5-2$ ) indicate comparable oceanic and atmospheric transports; cross-hatched areas ( $<0.5$ ) represent atmospheric dominance

Atlantic Ocean's up-net radiation gradient heat transfer. Thus, southward atmospheric transports should be larger in magnitude than the total values to satisfy required heat balance. By contrast, the atmospheric transports in the southern Indian Ocean must be smaller than the total required values because of poleward heat transports within the ocean. Therefore, as given by the model, maximum heat transports within the atmosphere should be found in the Atlantic Ocean, and because of the contrasted roles of the atmosphere in the two ocean basins, strong zonal asymmetries are expected.

It has been pointed out that the magnitudes of the total east-west energy transports are about 30% of the north-south transports in tropical latitudes (Sohn and Smith, 1992a). From an inter-comparison of the oceanic and atmospheric transports given in Figs. 5a and 5b, it is evident that the major cross-meridional fluxes over the tropics take place within the ocean. As further indicated in Sohn and Smith (1992a), energy deficits over interior tropical and subtropical land areas are offset by zonal atmospheric components. This is because low latitude land areas, which are source regions in the north-south framework, are energy deficit regions in an east-west sense.

In order to examine in more detail the role of

the oceans in the east-west framework, Fig. 6 has been prepared which shows the ratio of the cross-meridional oceanic transport component to the corresponding atmospheric component. Dominant cross-meridional oceanic transports are found over the eastern part of the Pacific, the central Indian Ocean, and over the north and equatorial regions of the Atlantic. Compared to the large area of dominant ocean transport over the tropics, only a small portion of the total ocean system, which mainly includes a small sector of the eastern Pacific off the Mexican coast along with the western Pacific sub-tropics, are dominated by the atmosphere. Since these portions of the Pacific are not part of the relatively strong east-west energy transport dipole regime (see Fig. 6 from Sohn and Smith, 1992a), these new results suggest that tropical cross-meridional energy transports are almost exclusively controlled by low latitude ocean currents.

#### 4. Discussion and Conclusions

In first part of this paper we provided evidence that the MEP principle applied to the atmosphere can serve as a governing rule on macroscale global climate. Moreover, we demonstrated that this principle can be used as a tool to parti-

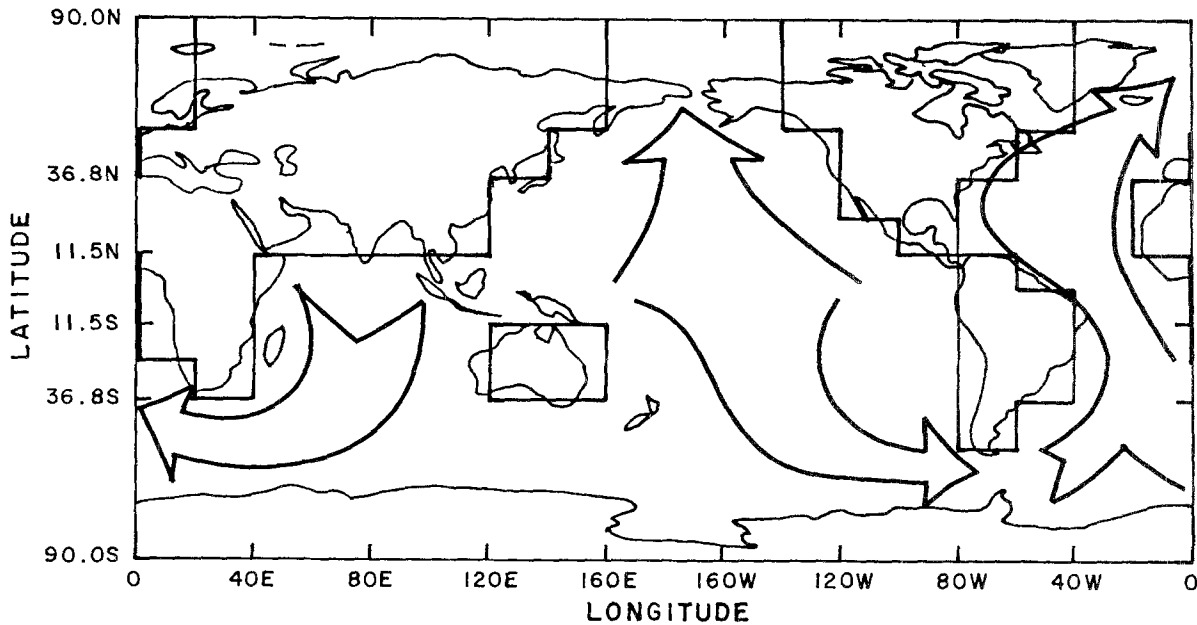


Fig. 7. Schematic depiction of general oceanic heat transport pattern based on the study of Stommel (1980)

tion the satellite-diagnosed total required energy transports into oceanic and atmospheric components. For the separation of two-dimensional ocean transports, we extended the one-dimensional MEP approach to an equally-divided, two-dimensional 180 box model. Results have demonstrated that the MEP principle reproduces generally-accepted features of oceanic heat transports as shown in the Fig. 7 map (based on Stommel, 1980), indicating northward transports throughout the Atlantic Ocean, southward transports throughout the Indian Ocean, and poleward transports in the separate hemispheres of the Pacific Ocean. The two-dimensional results in the Atlantic and Indian Ocean basins show qualitative agreement to previously reported features based on the both direct and indirect estimates, although there is so much disparity between the previously published results, it is difficult to carry out an absolute quantitative validation. By the same token, it appears that the magnitudes of the ocean transports found for the North Atlantic are too small in light of the Hall and Bryden (1982) and Roemmich and Wunch (1985) studies, which are solid points of reference for the  $24^{\circ}\text{N}$  and  $36^{\circ}\text{N}$  transects. In turn, we obtain transports in the North Pacific which are larger than suggested by various past estimates, although the estimates for this basin are generally less reliable than

the Atlantic. The smaller oceanic transports in the North Atlantic are partly the result of the limited spatial resolution of the 180-box model which cannot correctly resolve continental-oceanic boundaries and thus cannot fully account for the coastal Florida Current and portions of the Gulf Stream. There is a relationship between the underestimates in the North Atlantic to the overestimates in the North Pacific since the ratios of total ocean transport to the required transports (as a function of latitude) obtained from the one-dimensional results have been used as optimization constraints. It should also be noted that the use of zonally symmetric model parameters may induce additional errors, although sensitivity tests did not indicate this to be a serious source of uncertainty with respect to the transports themselves. Therefore, the major source of discrepancy in the northern hemisphere is thought to be due to the resolution of the land-sea boundaries. A higher resolution grid mesh with better knowledge of the zonally dependent model parameters would likely improve the results, although the degree of improvement may not be quantifiable on a global basis until a more reliable global data set based on direct estimates becomes available.

It is worth noting that these results are substantially different from those of Paltridge (1978). He applied the MEP principle to the two-dimen-

sional earth-atmosphere system and calculated zonal and meridional components of atmospheric and oceanic energy fluxes by assuming that the rate of dissipation of energy in the atmosphere and ocean are identical. His approach did not replicate the generally accepted oceanic transport features, e.g. northward transports in the South Atlantic and southward transports in the Indian Ocean. Instead, his solution exhibited poleward transports separated along the equator within all three ocean basins mimicking the total required transport pattern such as given in Fig. 3. Furthermore, the basic magnitudes of the total transports were less than half those that would be calculated directly from knowledge of the global net radiation balance.

There has been a long-term debate about the role of the South Pacific in carrying out heat transports based on differences between indirect methods and the direct oceanographic calculations (see Table 3). Since the results generated by the MEP approach are generally consistent with the direct calculations in that basin, we favor the argument which suggests that the South Pacific exerts weak control on redistributing energy poleward. In addition, the two-dimensional calculations help identify heat exchange features between and within oceans. Heat deficits in the southern hemisphere Atlantic Ocean induced by northward heat transports at high latitudes, tend to be offset by cross-meridional transports from the Pacific and Indian Oceans through inter-ocean heat exchange, although the magnitudes appear small. More importantly, it has been shown that cross-meridional heat transports in low latitudes are dominated by the oceans.

The corresponding two-dimensional atmospheric transports show much larger poleward transports over the mid-latitude continental areas than those over the oceans at the same latitude. Another dominant feature in the atmospheric transports is strong zonal asymmetry in the southern hemisphere. This result suggests that heat transport processes are not consistent with what we might expect from the generally zonally symmetric distribution of dynamic and thermodynamic variables. In contrast to the weak cross-equatorial atmospheric fluxes found in the zonally averaged results of Part I, significant cross-equatorial atmospheric transports are found in the three ocean basins with near-zero transports over land. Thus

the atmospheric cross-equatorial energy flux from the southern hemisphere to the northern hemisphere in the Indian Ocean is largely compensated by the center cross-equatorial energy flux by the Pacific and Atlantic Oceans, resulting in the near-zero exchange in the zonally averaged solution.

Since we have been able to reproduce generally known features in the general circulations of the oceans and atmosphere, our study suggests that the modeling methodology is a sound way to separate two-dimensional ocean/atmosphere transports from conventional satellite measurements of net radiation. This provides an independent means to assess the direct techniques based on in situ ocean measurements and the indirect techniques based on residual calculations within a surface energy budget framework. Although some caution must be used in interpreting the transport magnitudes given the current grid resolution, the use of zonally-averaged model constants, and the current optimization constraints, all of these model features could be refined with the expectation that the solution accuracy would improve.

#### Acknowledgements

We express our appreciation to Dr. Martin Berger of Tel Aviv University, and Dr. Michael Navon of Florida State University (FSU) for their advice in solving the optimization problem that arose in this study. This research has been supported under NASA Grant NAGW-1840. Computations were performed on both the ETA-10G and Cray-YMP located at Florida State University (FSU). A portion of the computational support has been provided by the Supercomputer Computations Research Institute at FSU under U.S. Department of Energy Contract DOE-FC05-85ER250000.

#### References

- Bennett, A. F., 1978: Poleward heat fluxes in southern hemisphere oceans. *J. Phys. Oceanogr.*, **8**, 785–798.
- Blazejewski, H., Cadet, D. L., Marsal, O., 1986: Low-frequency sea surface temperature and wind variations over the Indian and Pacific Oceans. *J. Geophys. Res.*, **91**, 5129–5132.
- Bryden, H. L., Roemmich, D. H., Church, J. A., 1991: Ocean heat transport across 24° N in the Pacific. *Deep-Sea Research*, **38**, 297–324.
- Bunker, A. F., 1976: Computation of energy flux and annual air-sea interaction cycles of the North Atlantic Ocean. *Mon. Wea. Rev.*, **104**, 1122–1140.
- Campbell, G. G., 1980: *Energy transport within the earth's atmosphere-ocean from a climate point of view*. Ph.D.

- Dissertation, Dept. of Atmos. Sci., Colorado State University, Fort Collins, CO 80523, 149 pp.
- Fu, L.-L., 1981: The general circulation and meridional heat transport of the subtropical South Atlantic determined by inverse methods. *J. Phys. Oceanogr.*, **11**, 1171–1193
- Fu, L.-L., 1986: Mass, heat and fresh water fluxes in the South Indian Ocean. *J. Phys. Oceanogr.*, **16**, 1683–1693.
- Georgi, D. T., Toole, J. M., 1982: The antarctic circumpolar current and oceanic heat and freshwater budget. *J. Marine Res.*, **40**, 183–197.
- Hall, M. M., Bryden, H. L., 1982: Direct estimates and mechanisms of ocean heat transport. *Deep-Sea Research*, **29**, 339–359.
- Hastenrath, S., 1982: On meridional heat transports in the world ocean. *J. Phys. Oceanogr.*, **12**, 922–927.
- Hsiung, J., 1985: Estimates of global oceanic meridional heat transport. *J. Phys. Oceanogr.*, **15**, 1405–1413.
- Levitus, S., 1992: *Climatological Atlas of the World Ocean*. NOAA Professional Paper No. 13 (U.S. GPO, Washington D.C.), 173 pp.
- North, G. R., Cahalan, R. F., Coakley, J. A. Jr., 1981: Energy balance climate models. *Rev. Geophys. Space Phys.*, **19**, 91–121.
- Oort, A. H., Peixóto, J. P., 1983: Global angular momentum and energy balance requirements from observations. *Adv. Geophys.*, **25**, 355–489.
- Paltridge, G. W., 1978: The steady-state format of global climate. *Quart. J. Roy. Meteor. Soc.*, **104**, 927–945.
- Paltridge, G. W., 1975: Global dynamics and climate – a system of minimum entropy exchange. *Quart. J. Roy. Meteor. Soc.*, **101**, 475–484.
- Rago, T. A., Rossby, H. T., 1987: Heat transport into the North Atlantic Ocean north of 32° N latitude. *J. Phys. Oceanogr.*, **17**, 854–871.
- Roemmich, D., McCallister, T., 1989: Large scale circulation of the North Pacific Ocean. *Prog. Oceanogr.*, **22**, 171–204.
- Roemmich, D., Wunsch, C., 1985: Two transatlantic sections: Meridional circulation and heat flux in the subtropical North Atlantic Ocean. *Deep-Sea Research*, **32**, 619–664.
- Sohn, B. J., Smith, E. A., 1993: Energy transports by ocean and atmosphere based on an entropy extremum principle. Part I: Zonal averaged transports. *J. Climate*, **6**, 886–899.
- Sohn, B. J., Smith, E. A., 1992a: Global energy transports and the influence of clouds on transport requirements – A satellite analysis. *J. Climate*, **5**, 717–734.
- Sohn, B. J., Smith, E. A., 1992b: The modulation of the low latitude radiation budget by cloud and surface forcing on interannual time scales. *J. Climate*, **5**, 831–846.
- Sohn, B. J., Smith, E. A., 1992c: The significance of cloud-radiative forcing to the general circulation on climate time scale – A satellite interpretation. *J. Atmos. Sci.*, **49**, 845–860.
- Stommel, H., 1980: Asymmetry of interoceanic fresh-water and heat fluxes. *Proc. U.S. Natl. Acad. Sci.*, **77**, 2377–2381.
- Stowe, L. L., Wellemeyer, C. G., Eck, T. F., Yeh, H. Y. M., The Nimbus-7 Cloud Data Processing Team, 1988: Nimbus-7 global cloud climatology. Part I: Algorithms and validation. *J. Climate*, **1**, 445–470.
- Talley, L. D., 1984: Meridional heat transport in the Pacific Ocean. *J. Phys. Oceanogr.*, **14**, 231–241.
- Toole, J. M., Raymer, M. E., 1985: Heat and fresh water budgets of the Indian Ocean – revisited. *Deep-Sea Research*, **32**, 917–928.
- Trenberth, K. E., 1981: Interannual variability of the Southern Hemisphere 500 mb flow: Regional characteristics. *Mon. Wea. Rev.*, **109**, 127–136.
- Wunsch, C., Hum, D., Grant, B., 1983: Mass, heat, salt and nutrient fluxes in the South Pacific Ocean. *J. Phys. Oceanogr.*, **13**, 725–753.

Author's address: Byung-Ju Sohn and Eric A. Smith, Department of Meteorology and Supercomputer Computations Research Institute, Florida State University, Tallahassee, FL 32306, U.S.A.